

Surface modification of aluminum alloy 6063 with trialkoxysilane solutions¹

A.M. Semiletov^{ID}* and Yu.I. Kuznetsov^{ID}

A.N. Frumkin Institute of Physical Chemistry and Electrochemistry, Russian Academy of Sciences, Leninsky pr. 31, 119071 Moscow, Russian Federation

**E-mail: semal1990@mail.ru*

Abstract

The superhydrophobic (SHP) films on metal surfaces are the most important class of multifunctional coatings with a number of useful properties: anti-corrosion, anti-fouling, self-cleaning and anti-icing. To obtain the anticorrosive SHP coatings, a method is used that combines a preliminary surface preparation with subsequent modification with a hydrophobic agent. It is important that the creation of a specific surface texture is a necessary condition for obtaining stable SHP coatings. In this article, we consider the possibility of obtaining the protective films of on a smooth and laser-textured surface of 6063 aluminum alloy. It is shown that the laser treatment of the alloy and subsequent modification in solutions of vinyltrimethoxysilane, octyltriethoxysilane, and octadecyltrimethoxysilane leads to SHP of the surface. The results degradation of SHP state of the alloy in water indicate a greater stability of the films formed from solutions of hydrophobic trialkoxysilanes: octyltriethoxysilane and octadecyltrimethoxysilane. The protective ability of SHP coatings was evaluated by polarization measurements, electrochemical impedance spectroscopy and corrosion test in a salt spray chamber. The electrochemical tests of the samples in a sodium chloride solution showed that the SHP films effectively prevented local depassivation. It has been established that SHP films formed from a solution of octadecyltrimethoxysilane have the best anticorrosive properties, and the time until the appearance of the first corrosion damage in a salt spray test is $\tau_{\text{cor}}=32$ days.

Received: January 6, 2022. Published: February 17, 2022

doi: [10.17675/2305-6894-2022-11-1-17](https://doi.org/10.17675/2305-6894-2022-11-1-17)

Keywords: *aluminum, corrosion, superhydrophobization, trialkoxysilanes.*

1. Introduction

Aluminum alloys are widely used as structural materials in many industries due to their good mechanical properties, thermal and electrical conductivity. However, in chloride-containing solutions, a marine and humid environment aluminum alloys are subjected to local corrosion [1, 2].

¹ The materials used in the article were obtained under the Fundamental Scientific Research Program of the State Academies of Sciences for 2013–2020: “Development of the fundamental scientific foundations of the protective effect of metal corrosion inhibitors in gas and condensed media, nanocomposites, paints and conversion coatings” (State registration number AAAA-A18-118121090043-0).

Previously, the methods based on the use very toxic of chromium (VI) compounds were used to protect of aluminum alloys from corrosion [3]. Therefore, many efforts have been made to develop non-toxic methods for protect of aluminum alloys: the application of conversion [4, 5] and organic coatings [6], corrosion inhibitors (CIs) [7–9].

Various trialkoxysilanes (TAS) can be used as potential CIs [10]. They can form self-organizing molecular layers on metal surfaces for corrosion protection [11].

The inhibition of metal corrosion by TAS is due to their interaction with the surface hydroxyl groups of metals leading to the formation of metallosiloxane covalent bonds –Si–O–Me– and polycondensation of neighboring molecules in the surface siloxane layer [12]. It is known [13, 14] that TAS are chemisorbed from aqueous solutions on the aluminum surface and to prevent general and local corrosion in chloride-containing media.

Despite the fact that TAS can be used as potential CIs, the main disadvantage of siloxane films over chromate coatings is the absence of the so-called “self-healing” effect of siloxanes. Numerous studies are aimed at eliminating this deficiency of silanes by introducing SiO₂ nanoparticles [15] and cerium (III) compounds [16, 17] into the siloxane film, which contribute to the “healing” of defects.

Recently, to increase the corrosion resistance of aluminum alloys the superhydrophobic (SHP) coatings have become widespread [18, 19]. It's known, to achieve the SHP state at the first stage a surface with a multimodal roughness is obtained, which is subsequently modified with perfluorinated TAS [20, 21].

In practice, the laser ablation is an effective method for the formation of microstructures on a metal surface [22, 23]. The shape and size of the microstructures can be varied by adjusting parameters of laser processing: laser power, frequency, pulse duration and processing speed. It was shown in [23] that after a laser treatment the periodic structure of aluminum oxide on the surface of the AMg3 aluminum alloy are formed. The subsequent modification of this surface in a decane solution of fluorosilane forms an SHP coating with a high contact angle $\Theta_c = 173.4^\circ$ and a small roll-off angle of 2.4° . In addition, the obtained SHP coating effectively inhibits the corrosion of the alloy in chloride solutions.

However, despite the success of the use of fluorinated TASs to achieve the SHP state, their practical use is limited not only by their toxicity, but also by high cost. An alternative fluorinated compounds can be application of cheap, fluorine-free and environmentally friendly TASs. This work reports the results of superhydrophobization of alloy 6063 surface from water and water–ethanol solutions of TAS for its corrosion protection in chloride media.

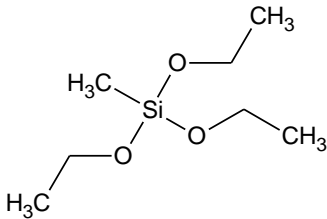
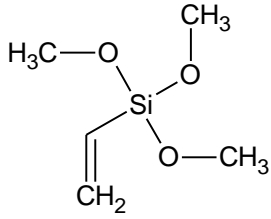
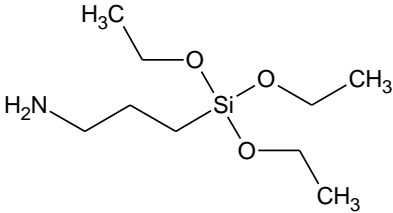
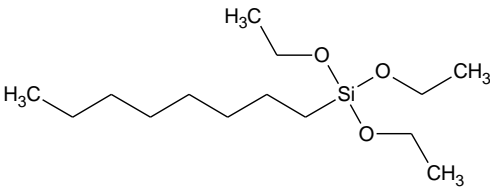
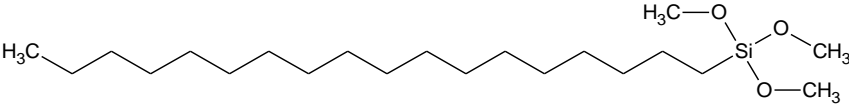
2. Experimental

2.1. Materials

The studies were carried out on 6063 aluminum alloy samples, content (wt%): Fe ≤ 0.35, Si 0.2–0.6, Mn ≤ 0.1, Cr ≤ 0.1, Ti ≤ 0.10, Cu ≤ 0.1, Mg 0.45–0.9, Zn ≤ 0.1, Al – the rest.

As hydrophobic agents, we used TAS solutions in water (methyltriethoxysilane (MTES, 97%, Penta-91), vinyltrimethoxysilane (VTMS, 97%, Penta-91), aminopropyltriethoxysilane (APTES, 99%, Penta-91)) and in a water–ethanol mixture (octyltriethoxysilane (OTES, 97.5%, Sigma Aldrich) and octadecyltrimethoxysilane (ODTMS, 90%, Sigma Aldrich)) (Table 1).

Table 1. Structural formulas of the TAS and $\lg P$ values.

TAS	Structural formula	$\lg P$
Methyltriethoxysilane (MTES)		1.73±0.42
Vinyltrimethoxysilane (VTMS)		3.12±0.66
Aminopropyltriethoxysilane (APTES)		1.37±0.44
Octyltriethoxysilane (OTES)		5.45±0.42
Octadecyltrimethoxysilane (ODTMS)		9.17±0.43

2.2 Preparation of SHP layers

The protective layers were studied on smooth and laser textured surfaces. In the first case, aluminum samples 30×40×2 mm in size were polished with emery paper of various grain sizes (up to 1500), degreased with ethanol, washed with distilled water, and dried in air for 60 min to form an oxide layer.

In the second case, to obtain a uniformly inhomogeneous rough surface, the samples were processed with an air-cooled fiber-optic laser marker XM-30 with the following

parameters of laser processing (LP): λ (wavelength) 1.064 μm , ν (radiation frequency) 20 kHz, d (laser beam diameter) 0.01 mm, l (distance between linear trajectories) 0.01 mm, v (speed of movement of the laser beam) 500 mm/s, W (laser power) 10 W. The treatment was carried out with two laser passes in the perpendicular direction to the surface, *i.e.* with obtaining a “mesh, cell” structure. Further, to remove the metal dust formed during the LP process, the samples were washed with ethanol and dried in air at $t = 65^\circ\text{C}$.

The hydrophobic treatment of alloy 6063 samples was carried out at room temperature $t = 20 \pm 2^\circ\text{C}$ for 1 h, then the samples were dried for 1 h with air at 150°C and washed with distilled water to remove physically adsorbed layers.

2.3 Optical microscopy

The micrographs of the alloy 6063 surface after mechanical polishing and LP were obtained using an optical microscope Biomed-3 equipped with a camera Levenhuk M1000PLUS at $\times 100$ magnification.

2.4 Water contact angle (Θ_c) measurements

The hydrophobic properties of the protective layers on an aluminum alloy formed from TAS solutions were evaluated by the value of the static contact angle Θ_c . To measure Θ_c the samples were placed in a laboratory setup with a built-in camera DCM 300 and a drop of distilled water ($3\text{--}5 \mu\text{l}$) was placed on the surface under study. Determination of Θ_c was carried out from photographic images of a drop using the Corel R.A.V.E. 2.0 image editor. To obtain reliable wetting characteristics, the initial Θ_c was measured 5–10 s after the droplet landing on 5 different areas of the surface of each sample. The average value of the angle was determined for 10 successive images of the drop.

The stability of the SHP properties of the coatings was estimated by the change in the Θ_c value with time during corrosion tests of samples in distilled water. The testing of samples, which lasted up to 70 days, the Θ_c measurements were carried out after 7, 14 and then every 14 days. The samples were removed from distilled water, dried at 150°C , Θ_c was determined, and then returned to the solution to continue testing.

2.5 Polarization measurements and EIS

The electrochemical studies of the protective properties of SHP films were carried out by the polarization (potentiodynamic) method. The polarization measurements were performed in 0.05 M NaCl solution with pH 6.5, using an IPC-Pro MF potentiostat with a potential scan rate of 0.002 V/s. The measured electrode potentials were converted to the normal hydrogen scale. A platinum wire was used as the auxiliary electrode. A two-key silver chloride electrode was used as the reference electrode. All electrochemical measurements were carried out under static conditions at room temperature of the solution and with natural aeration.

To avoid damage of the SHP film formed on the surface of alloy 6063, the electrode was not kept in the solution until E_{cor} was established. The resistance of alloy 6063 coated with SHP films to the corrosive action of chloride ions was evaluated by the difference of the local depassivation potentials, $\Delta E_{\text{pt}} = E_{\text{pt}}^{\text{SHP}} - E_{\text{pt}}^{\text{LT}}$, which were determined from the anodic polarization curves on samples after laser treatment ($E_{\text{pt}}^{\text{LT}}$) and with preliminary modification with SHP agents ($E_{\text{pt}}^{\text{SHP}}$).

Electrochemical impedance spectroscopy (EIS) was performed using an Autolab PGSTAT302 potentiostat with an FRA32M module. The impedance spectra were recorded in the frequency range f from 10 kHz to 0.1 Hz with AC voltage amplitude of 10 mV. Test electrodes were prepared similarly to samples for contact angle and polarization measurements. The results were processed using NOVA 2.1.4 software. The experimental data were in agreement with the calculated data at least 95%.

2.6 Corrosion tests

The corrosion tests of aluminum samples with coatings of CIs were carried out in a salt spray chamber (SSC) Weiss SC/KWT 450. The 5% NaCl (pH 6.9) was used as a salt solution in the SSC. The chamber operated continuously in a cyclic mode (one cycle – 15 minutes of spraying the salt solution, then the chamber was turned off for 45 minutes, then the cycle was repeated). The tests were carried out at $t = 35^\circ\text{C}$ and 100% humidity. Inspection of the samples was carried out 3 times a day from the beginning of the tests to determine the time until the appearance of the first corrosion damage τ_{cor} .

3. Results and Discussion

3.1 Surface morphology of alloy 6063

Figure 1 shows micrographs of the surface of alloy 6063 subjected to mechanical polishing and LP. In the photograph of the smooth surface, there are small surface defects and traces of mechanical polishing (a). After LP, a rough uniformly inhomogeneous structure (b) is formed on the surface, and according to the results of profilometric measurements, the height of irregularities in the selected LP mode does not exceed 8–12 μm [24].

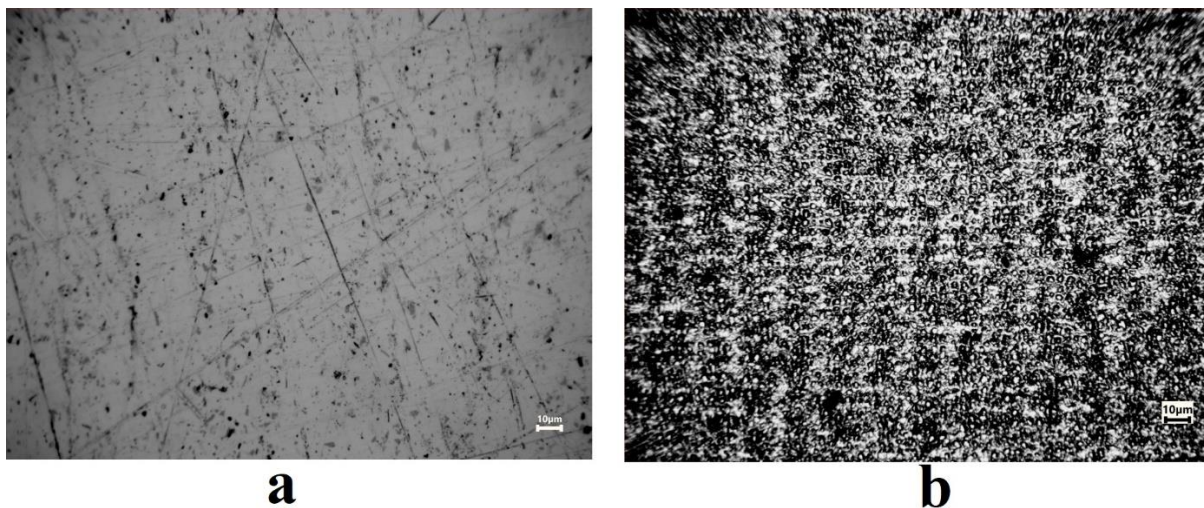


Figure 1. Micrographs of the alloy 6063 surface after mechanical polishing (a) and LP (b).

3.2 The effect of laser treatment of surface on hydrophobic properties of the layers formed from TAS solutions

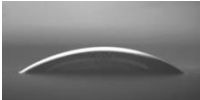
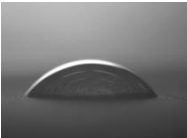
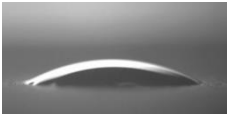

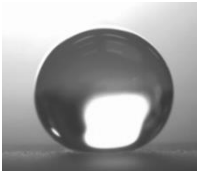


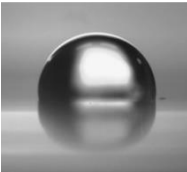
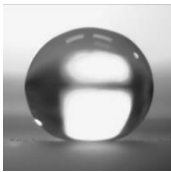

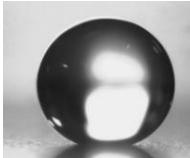
The adsorption activity of organic compounds depends on hydrophobicity, which can be quantitatively characterized by the logarithm of the distribution coefficient ($\lg P$) of a substance in a system of two immiscible liquids, octanol–water. The value of $\lg P$ is a characteristic of the hydrophobicity of neutral molecules, and can be obtained both experimentally and by calculation, using hydrophobicity f -constants of substituents [25].

The values of $\lg P$ for the studied TAS, calculated using the “ACDLABS 12.0” software, can be arranged in the series $\text{APTES} < \text{MTES} < \text{VTMS} < \text{OTES} < \text{ODTMS}$ (Table 1), thus confirming the highest hydrophobicity of ODTMS molecules, which is even higher than that of octadecylphosphonic acid, $\lg P = 7.01 \pm 0.44$ [26].

The smooth surface of alloy 6063 after mechanical polishing is hydrophilic and characterized by a low value of $\Theta_c = 26^\circ$. The modification of the surface in solutions of MTES, AEAPTS and VTMS, possibly from aqueous solutions, due to their good solubility in water at $C = 10$ mM. However, the treatment of samples only in a VTMS solution leads to hydrophobization, and $\Theta_c = 97^\circ$ (Table 2). The surface modification in MTES and AEAPTS solutions is less effective, and the contact angle does not exceed 50° .

Because of the limited water solubility of TAS with a long alkyl chain, OTES and ODTMS, their water–ethanol solutions were used for surface modification (the water/ethanol volume ratio was 1:1 for OTES and 1:9 for ODTMS). Treatment of the samples with an OTES solution leads to surface hydrophobization, $\Theta_c = 101^\circ$, and modification with an ODTMS solution increases the value of Θ_c to 105° . Thus, the efficiency of the studied TASs in achieving the hydrophobic state is consistent with the calculated series of $\lg P$.

Table 2. The values of contact angles (Θ_c) and images of water droplets on smooth and textured surfaces of aluminum alloy 6063 samples modified in TAS solutions.

Treatment	Θ_c , degree	
	smooth surface	textured surface
Without treatment	 $26 \pm 3^\circ$	— $0 \pm 2^\circ$
MTES	 $50 \pm 2^\circ$	 $30 \pm 3^\circ$
VTMS	 $97 \pm 2^\circ$	 $155 \pm 3^\circ$
AEAPTS	 $42 \pm 2^\circ$	 $10 \pm 2^\circ$
OTES	 $101 \pm 2^\circ$	 $157 \pm 2^\circ$
ODTMS	 $105 \pm 2^\circ$	 $160 \pm 3^\circ$

For achieving the SHP state, it is necessary to take into account the surface morphology. Indeed, after LP and subsequent treatment of samples in an aqueous solution of VTMS, the surface becomes superhydrophobic, and $\Theta_c = 155^\circ$. Treatment in solutions of MTES and AEAPTS not only does not lead to surface superhydrophobization but even reduces the values of contact angles obtained on a smooth surface. Modification of samples in OTES and ODTMS solutions is more effective and gives $\Theta_c = 157^\circ$ and 160° , respectively.

3.3 The stability of superhydrophobic silane coatings

To assess the effectiveness of SHP coatings and the possibility of their practical application, it is important that they retain their properties in an aqueous environment.

The coating degradation was evaluated by the exposure of the samples in distilled water for 70 days (Figure 2). For samples with VTMS films, the SHP state persists for 7 days of testing, then the value Θ_c decreases, but after 14 days of exposure to water, the highly hydrophobic state remains $\Theta_c=148^\circ$. Further, in time a decrease of the Θ_c occurs and after 70 days of exposure the surface loses hydrophobic properties.

The stability of films formed by TAS with a long alkyl radical is higher in aqueous solution. The SHP state of samples with OTES films is retained for 21 days, and ODTMS – 28 days. Further exposure of the samples leads to a decrease of the values Θ_c , however, even after 70 days of testing in water, the surface remains hydrophobic.

It is important that the degradation of SHP properties of TAS films is uneven. Therefore, after 20 days of testing on the samples single corrosion damage is observed, even with saving of the SHP properties on many areas of the surface.

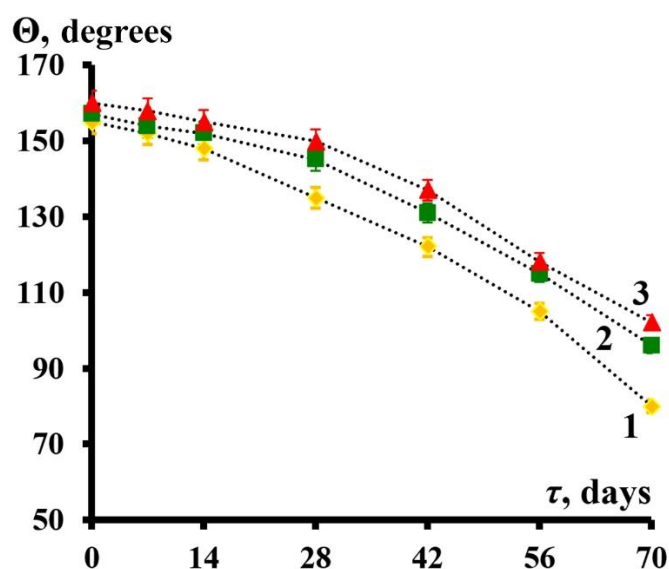


Figure 2. The evolution of contact angle Θ_c on alloy 6063 from the time of exposure of the samples in water, previously subjected to LP, and then modified in ethanol solutions containing 10 mM TAS: 1 – VTMS; 2 – OTES; 3 – ODTMS.

3.4 Electrochemical behavior of alloy 6063 modified with TAS

The high protective ability of SHP coatings for a long time in an aqueous solution suggests that it can be effective in the depassivation by chloride anions. In Figure 3 shows the anodic polarization curves of alloy 6063 in 0.05 M NaCl with pH 6.5. The initial potential of aluminum electrode in the test solution is $E=-0.55$ V, after anodic polarization a slight increase in current density $i_a=2-3 \mu\text{A}/\text{cm}^2$ occurs, but then, at $E_{pt}=-0.47$ V, a rapid i_a increase is observed, indicating the formation of pits on the surface.

Preliminary LP of the electrode leads to a change in E to -0.74 V, but the potential of local depassivation changes insignificantly to $E_{pt} = -0.45$ V. However, if such an electrode after LP is treated with an ethanolic solution containing 10 mM VTMS, then its E_{cor} reaches -0.57 V, while E_{pt} increases to -0.35 V.

As expected, treatment of the textured surface of alloy 6063 with OTES and ODTMS solutions is more efficient, with $E_{pt} = -0.07$ and -0.01 V, and the values of ΔE are 0.40 and 0.46 V, respectively. Consequently, a high stability of the SHP surface can also be detected by the ability of the electrode to be more resistant to local depassivation by chlorides when recording anodic polarization curves.

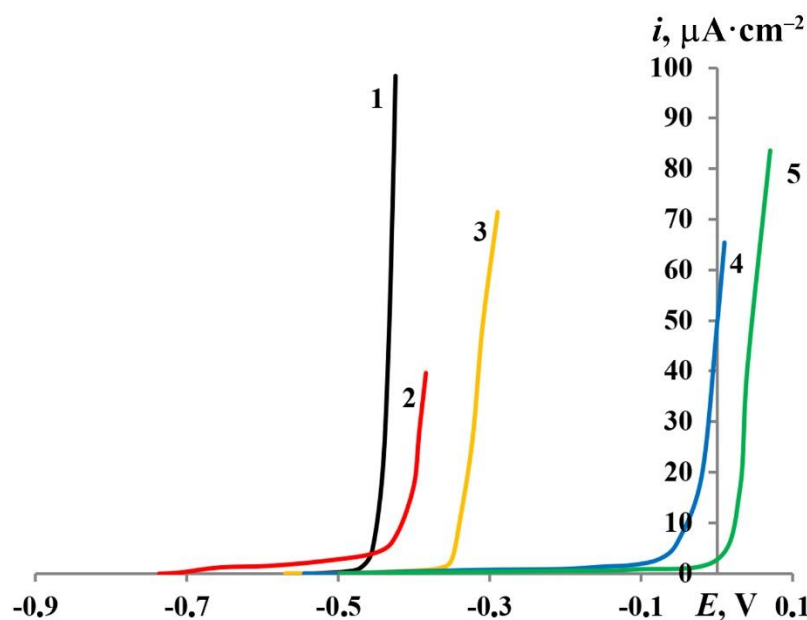


Figure 3. Anodic polarization curves of 6063 alloy in a 0.05 M NaCl solution without (1) and with preliminary LP (2) and then treated in TAS solutions ($C = 10$ mM): 3 – VTMS; 4 – OTES; 5 – ODTMS.

Additional information about the interaction of TAS (on the example of VTMS and ODTMS) with the surface of alloy 6063 can be obtained using the EIS method. The equivalent circuits used to describe the results of EIS are shown in Figure 4 (a – for an electrode subjected to LP, b – for an electrode subjected to LP and covered with VTMS and ODTMS films). The circuits contain the following elements: R_s – solution resistance; Q_{dl} and n_{dl} are the parameters of the constant phase element (CPE 1) describing the capacitance of the electric double layer; R_p – polarization resistance; Q_f and n_f – parameters of CPE 2 describing the capacitance of the surface film; R_f is the film resistance.

The results of measuring the EIS confirm the higher protective efficiency of the ODTMS (Figure 5). On the Nyquist plots, one can observe an increase in the radius of the hodographs obtained on the treated electrodes, in comparison with the untreated samples. The obtained values of the capacitance of the protective film (Table 3) show that it is higher in the case of VTMS than for ODTMS, but the resistance is higher for ODTMS. At the same

time, the polarization resistance increases from VTMS to ODTMS. This indicates an undoubtedly higher protective effect of the ODTMS coating than that of VTMS.

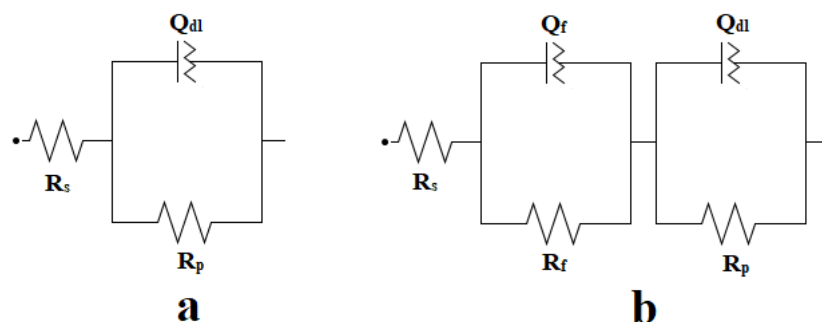


Figure 4. Electrical equivalent circuits used to describe the experimental EIS results.

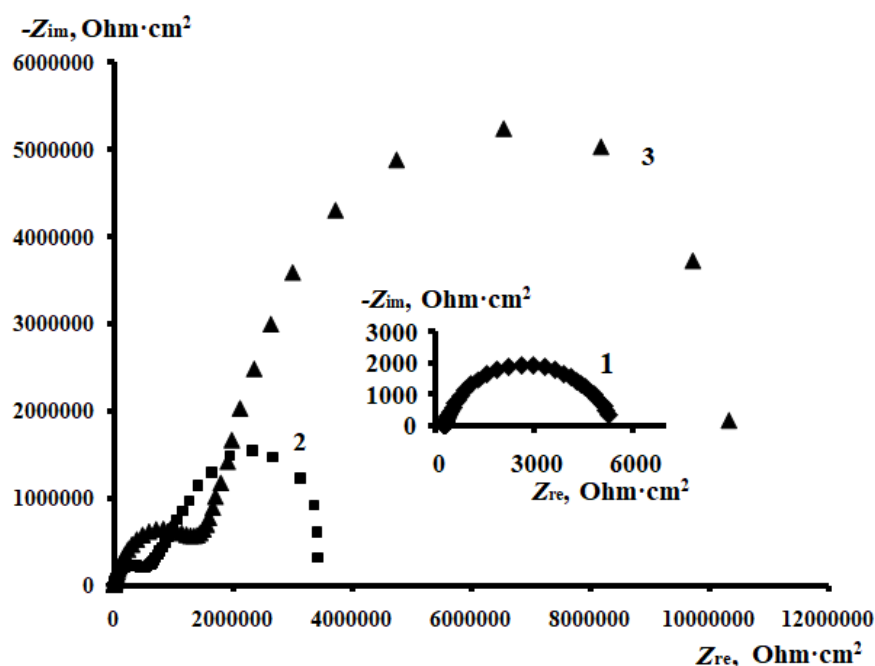


Figure 5. Nyquist plots obtained in a 0.05 M NaCl solution on alloy 6063 after LP (1) and subsequent treatment with VTMS (2) and ODTMS (3) solutions.

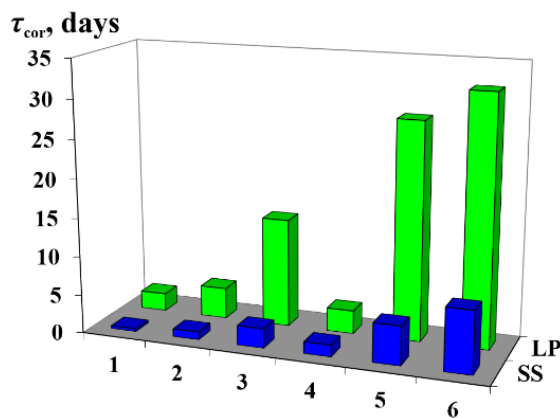
3.5 Results of corrosion tests in an SSC

On samples of alloy 6063 in an SSC, the first corrosion damage is observed after 8 hours of testing (Figure 6). The results of corrosion tests show a low protective ability of TAS films on a smooth surface. The surface modification with aqueous solutions of MTES and APTES $C=10$ mM leads to increase $\tau_{\text{cor}}=1-1.5$ days. Treatment in an aqueous solution of VTMS turns out to be more effective, and $\tau_{\text{cor}}=2.5$ days. The surface modification in water–ethanol solutions of hydrophobic TASs demonstrates better protective properties, for OTES $\tau_{\text{cor}}=5$ days, and ODTMS $\tau_{\text{cor}}=8$ days, respectively.

Table 3. Calculated parameters of the equivalent electrical circuits for alloy 6063 with SHP coatings of VTMS and ODTMS.

Parameter	Treatment		
	LP	LP – VTMS	LP – ODTMS
R_f (Ohm · cm ²)	–	$6.04 \cdot 10^5$	$1.65 \cdot 10^6$
Q_f (S · s ⁿ /cm ²)	–	$8.89 \cdot 10^{-6}$	$5.56 \cdot 10^{-6}$
n_f	–	0.556	0.607
R_p (Ohm · cm ²)	5181.7	$3.57 \cdot 10^6$	$9.58 \cdot 10^6$
Q_{dl} (S · s ⁿ /cm ²)	$7.66 \cdot 10^{-6}$	$2.09 \cdot 10^{-8}$	$1.40 \cdot 10^{-9}$
n_{dl}	0.874	0.973	0.927

Laser texturing of the surface increases the anti-corrosion resistance of alloy 6063, τ_{cor} = 2.3 days. Subsequent treatment in solutions of MTES and APTES leads to an increase in τ_{cor} , but their efficiency is low, τ_{cor} = 3–4 days. The SHP films formed from VTMS solution protect the alloy surface from corrosion for 14 days. Surface modification with OTES and ODTMS solutions is more effective not only according to polarization measurements and the kinetics of degradation of SHP properties, but also under SSC conditions. In fact, for OTES films, the time until the first corrosion damage on alloy 6063 is 28 days, while for ODTMS layers it is more than 32 days.

**Figure 6.** Time until the appearance of the first corrosion damage (τ_{cor}) in the SSC on smooth samples (SS) and LP alloy 6063 samples (1) modified in ethanol solutions of TAS: 2 – MTES; 3 – VTMS; 4 – APTES; 5 – OTES; 6 – ODTMS.

Conclusions

1. A method for the preparation of SHP coatings on an aluminum alloy 6063 surface, based on the laser treatment and followed modification in TAS solutions, is proposed. According to the efficiency in achieving the SHP state of the alloy, the studied TASs can be arranged in the row VTMS < OTES < ODTMS, which correlates to calculated values of $\lg P$.

2. There is a gradual degradation of the SHP properties of coatings in water; for OTES and ODTMS the SHP state persists for 28 days exposure of samples in water.
3. The electrochemical tests of 6063 alloy samples in a chloride solution showed that the OTES and ODTMS coatings effectively prevent local depassivation. The EIS results confirm the polarization measurements, showing a significant increase in the corrosion resistance of the alloy after adsorption of TAS, with a great advantage of ODTMS.
4. The results of corrosion tests in SSC indicate the high protective properties of SHP layers. On 6063 alloy samples covered by SHP coating of ODTMS the first corrosion damage is observed after 32 days.

References

1. W.L. Zhang and G.S. Frankel, Transitions between pitting and intergranular corrosion in AA2024, *Electrochim. Acta*, 2003, **48**, no. 9, 1193–1210. doi: [10.1016/S0013-4686\(02\)00828-9](https://doi.org/10.1016/S0013-4686(02)00828-9)
2. L.L. Liu, Q.L. Pan, X.D. Wang and S.W. Xiong, The effects of aging treatments on mechanical property and corrosion behavior of spray formed 7055 aluminium alloy, *J. Alloys Compd.*, 2018, **735**, 261–276. doi: [10.1016/j.jallcom.2017.11.070](https://doi.org/10.1016/j.jallcom.2017.11.070)
3. M.W. Kendig and R.G. Buchheit, Corrosion inhibition of aluminum and aluminum alloys by soluble chromates, chromate coatings, and chromate-free coatings, *Corrosion*, 2003, **59**, no. 5, 379–400. doi: [10.5006/1.3277570](https://doi.org/10.5006/1.3277570)
4. H.H. Zhang, X.F. Zhang, X.H. Zhao, Y.M. Tang and Y. Zuo, Preparation of Ti-Zr-Based conversion coating on 5052 aluminum alloy, and its corrosion resistance and antifouling performance, *Coatings*, 2018, **8**, no. 11, 397–407. doi: [10.3390/coatings8110397](https://doi.org/10.3390/coatings8110397)
5. A.S. Koryakin, Yu.A. Kuzenkov, S.V. Oleinik and V.L. Voititskii Chromium-free conversion protective coatings on 1424 aluminum alloy, *Prot. Met. Phys. Chem. Surf.*, 2020, **56**, 1305–1310. doi: [10.1134/S2070205120070096](https://doi.org/10.1134/S2070205120070096)
6. J. Telegdi, G. Luciano, S. Mahanty and T. Abohalkuma, Inhibition of aluminum alloy corrosion in electrolytes by self-assembled fluorophosphonic acid molecular layer, *Mater. Corros.*, 2016, **67**, no. 10, 1027–1033. doi: [10.1002/maco.201508792](https://doi.org/10.1002/maco.201508792)
7. K. Xhanari and M. Finsgar, Organic corrosion inhibitors for aluminum and its alloys in chloride and alkaline solutions: A review, *Arabian J. Chem.*, 2019, **12**, no. 8, 4646–4663. doi: [10.1016/j.arabjc.2016.08.009](https://doi.org/10.1016/j.arabjc.2016.08.009)
8. A. Balbo, A. Frignani, V. Grassi and F. Zucchi, Corrosion inhibition by anionic surfactants of AA2198 Li-containing aluminium alloy in chloride solutions, *Corros. Sci.*, 2013, **73**, 80–88. doi: [10.1016/j.corsci.2013.03.027](https://doi.org/10.1016/j.corsci.2013.03.027)
9. A.M. Semiletov, A.A. Chirkunov and Yu.I. Kuznetsov, Protection of D16 alloy against corrosion in neutral aqueous solutions and in an aggressive atmosphere using organic inhibitors, *Prot. Met. Phys. Chem. Surf.*, 2020, **56**, 1285–1292. doi: [10.1134/S2070205120070163](https://doi.org/10.1134/S2070205120070163)

10. M.A. Petrunin, N.A. Gladkikh, M.A. Maleeva, L.B. Maksaeva and T.A. Yurasova, The use of organosilanes to inhibit metal corrosion, *Int. J. Corros. Scale Inhib.*, 2019, **8**, no. 4, 882–907. doi: [10.17675/2305-6894-2019-8-4-6](https://doi.org/10.17675/2305-6894-2019-8-4-6)
11. H. Sugimura, A. Hozumi, T. Kameyama and O. Takai, Organosilane self-assembled monolayers formed at the vapour/solid interface, *Surf. Interface Anal.*, 2002, **34**, 550–554. doi: [10.1002/sia.1358](https://doi.org/10.1002/sia.1358)
12. E.P. Plueddenmann, *Silane Coupling Agents*, 2nd edition, New York: Plenum Press, 1991, 181.
13. M.A. Petrunin, L.B. Maksaeva, T.A. Yurasova, E.V. Terekhova, V.A. Kotenev and A.Yu. Tsivadze, Adsorption of alkoxysilanes on aluminum surface from aqueous solutions, *Prot. Met. Phys. Chem. Surf.*, 2013, **49**, 655–661. doi: [10.1134/S2070205113060117](https://doi.org/10.1134/S2070205113060117)
14. A.M. Beccaria and L. Chiaruttini, The inhibitive action of metacryloxypropylmethoxysilane (MAOS) on aluminium corrosion in NaCl solutions, *Corros. Sci.*, 1999, **41**, no. 5, 885–899. doi: [10.1016/S0010-938X\(98\)00161-9](https://doi.org/10.1016/S0010-938X(98)00161-9)
15. V. Palanivel, D. Zhu and W.J. van Ooij, Nanoparticle-filled silane films as chromate replacements for aluminum alloys, *Prog. Org. Coat.*, 2003, **47**, no. 3–4, 384–392. doi: [10.1016/j.porgcoat.2003.08.015](https://doi.org/10.1016/j.porgcoat.2003.08.015)
16. M.L. Zheludkevich, R. Serra, M.F. Montemor, K.A. Yasakau, I.M.M. Salvado and M.G.S. Ferreira, Nanostructured sol–gel coatings doped with cerium nitrate as pretreatments for AA2024-T3: Corrosion protection performance, *Electrochim. Acta*, 2005, **51**, no. 2, 208–217. doi: [10.1016/j.electacta.2005.04.021](https://doi.org/10.1016/j.electacta.2005.04.021)
17. L.E.M. Palomino, P.H. Suegama, I.V. Aokia, Z. Pászti and H.G. de Melo, Investigation of the corrosion behaviour of a bilayer cerium-silane pre-treatment on Al 2024-T3 in 0.1 M NaCl, *Electrochim. Acta*, 2007, **52**, no. 27, 7496–7505. doi: [10.1016/j.electacta.2007.03.002](https://doi.org/10.1016/j.electacta.2007.03.002)
18. D. Zhang, L. Wang, H. Qian and X. Li, Superhydrophobic surfaces for corrosion protection: a review of recent progresses and future directions, *J. Coat. Technol. Res.*, 2016, **13**, 11–29. doi: [10.1007/s11998-015-9744-6](https://doi.org/10.1007/s11998-015-9744-6)
19. J.T. Simpson, S.R. Hunter and T. Aytug, Superhydrophobic materials and coatings: a review, *Rep. Prog. Phys.*, 2015, **78**, 086501. doi: [10.1088/0034-4885/78/8/086501](https://doi.org/10.1088/0034-4885/78/8/086501)
20. Z. Lu, P. Wang and D. Zhang, Super-hydrophobic film fabricated on aluminium surface as a barrier to atmospheric corrosion in a marine environment, *Corros. Sci.*, 2015, **91**, 287–296. doi: [10.1016/j.corsci.2014.11.029](https://doi.org/10.1016/j.corsci.2014.11.029)
21. L.B. Boinovich and A.M. Emelyanenko, Hydrophobic materials and coatings: principles of design, properties and applications, *Russ. Chem. Rev.*, 2008, **77**, 583–600.
22. G.V. Redkina, A.S. Sergienko and Yu.I. Kuznetsov, Hydrophobic and anticorrosion properties of thin phosphonate–siloxane films formed on a laser textured zinc surface, *Int. J. Corros. Scale Inhib.*, 2020, **9**, no. 4, 1550–1563. doi: [10.17675/2305-6894-2020-9-4-23](https://doi.org/10.17675/2305-6894-2020-9-4-23)

-
23. L.B. Boinovich, E.B. Modin, A.R. Sayfutdinova, K.A. Emelyanenko, A.L. Vasiliev and A.M. Emelyanenko, Combination of functional nanoengineering and nanosecond laser texturing for design of superhydrophobic aluminum alloy with exceptional mechanical and chemical properties, *ACS Nano*, 2017, **11**, 10113–10123. doi: [10.1021/acsnano.7b04634](https://doi.org/10.1021/acsnano.7b04634)
 24. A.M. Semiletov, A.A. Kudelina and Yu.I. Kuznetsov, Anticorrosion and hydrophobic properties of carbonic acid films on surface of D16 aluminum alloy, *Korrozi.: Mater., Zashch. (Corrosion: materials, protection)*, 2021, no. 5, 23–29 (in Russian). doi: [10.31044/1813-7016-2021-0-5-23-29](https://doi.org/10.31044/1813-7016-2021-0-5-23-29)
 25. C. Hanch and A. Leo, *Substituent Constants for Correlation Analysis in Chemistry and Biology*, Wiley-Interscience: New York, 1979, 339.
 26. A.M. Semiletov, Yu.I. Kuznetsov, A.A. Chirkunov, I.A. Arkhipushkin and L.P. Kazanskii, Surface modification of the AD31 alloy by octadecylphosphonic acid for protection from atmospheric corrosion, *Korrozi.: Mater., Zashch. (Corrosion: materials, protection)*, 2020, no. 5, 13–20 (in Russian). doi: [10.31044/1813-7016-2020-0-5-13-20](https://doi.org/10.31044/1813-7016-2020-0-5-13-20)

